Experiments on the Temperature Profile and Cloud Thickness Inversion in Cirrus Cloudy Atmospheres

HWA-YOUNG YEH AND KUO-NAN LIOU

Department of Meteorology
University of Utah
Salt Lake City, Utah 84112, U. S. A.

(Manuscript received 26 January 1979, in final form 14 March 1979)

ABSTRACT

A modified relaxation method for inversion has been developed on the basis of the parameterized infrared transfer equation applicable to cirrus cloudy atmospheres. The method is then utilized for the simultaneous retrieval of the temperature profile and cloud thickness in atmospheres containing cirrus clouds. Numerical analyses and retrieval experiments have been carried out by using the Nimbus 6 High Resolution Infrared Sounder Data in which both longwave and shortwave channels in the carbon dioxide band are included. The retrieved results are physically discussed and numerically compared with the radiosonde observations. Comparisons reveal that the recovered temperature profiles in thin cirrus conditions agree reasonably well with the observed values. However, for cases when middle and/or low clouds are present, the recovered temperature profiles show considerable fluctuations, and the accuracy of the estimated cloud thickness is questionable.

1. Introduction

Although the nonuniqueness of the inversion problem using the infrared radiances sensed by satellites introduces difficulties in the determination of the atmospheric composition, numerical recovery of the temperature profile in recent years has proven to be successful. Accurate temperature profiles have been derived for clear atmospheric conditions (Chahine, 1970; Smith, 1970). Moreover, numerical procedures utilizing two adjacent fields of view for the recovery of temperature profiles in cloudy atmospheres have also been proposed by Smith *et al.* (1970) and Chahine (1974). None of these important investigations, however, has addressed the problem associated with high, semi-transparent cirrus clouds which contain nonspherical ice crystals of various sizes, possibly having preferred orientations in the atmosphere. It has been noted that the presence of cirrus clouds introduces serious difficulties in the retrieval of temperature and humidity profiles and surface conditions.

Occupying the upper troposphere and occasionally extending to the lower stratosphere, cirrus clouds are global in nature. Although thin cirrus are frequently invisible from the ground stations, they significantly interact with the thermal infrared radiation emitted from the earth. Owing to the complexity of the cloud interaction with the infrared radiation field of the atmosphere, information content of the temperature profile in the observed upwelling

radiance is difficult, if not impossible, to recover. Recently, Liou and Yeh (1979) have demonstrated some possibilities of deriving the cloud thickness and temperature profile employing the synthetic radiance data. It is the purpose of this study to explore further the theoretical foundation and numerical technique for the simultaneous determination of the temperature profile and cloud property in cirrus cloudy atmospheres.

In Section 2, we present the basic formulation of the upwelling radiance in cirrus cloudy atmospheres and the modified relaxation method for the reconstruction of the clear column radiation in cirrus conditions. Numerical experiments and a number of case studies utilizing the Nimbus 6 High Resolution Infrared Sounder (HIRS) data for the cloud thickness and temperature profile retrieval are then described and physically discussed.

2. Basic Formulation for Remote Sounding of Cloudy Atmospheres

Consider an overcast cirrus cloudy atmosphere in which the upwelling radiance at the top of the atmosphere may be theoretically expressed by (Liou, 1977)

$$I_i(\infty)=\tau_i^c(\Delta z)I_i(z_b)\tau_i(\infty,z_b+z)\Delta z + \int_{z_b+\Delta z}^{\infty} B_i[T(z)]d\tau_i(\infty,z), \quad (1)$$

Where i denotes the spectral channel, τ_i is the clear column transmittance in reference to the top of the atmosphere, z_b the cirrus cloud base height, Δz the cloud thickness, $B_i(T)$ the Planck function of a temperature T, and the cloud transmissivity τ_i^c (Δz) is defined as the ratio of the upwelling radiance at the cloud top; i.e., $I_i(z_b + \Delta z)$, to that at the cloud base $I_i(z_b)$, and it can be written in the form

$$\tau_i^c(\Delta z)=I_i(z_b+\Delta z)/I_i(z_b). \quad (2)$$

The upwelling radiance reaching the cloud base is given by

$$I_i(z_b)=B_i(T_s)\tau_i(z_b,0) + \int_0^{z_b} B_i[T(z)]d\tau_i(z_b,z), \quad (3)$$

Where T_s is the surface temperature and $\tau_i(z_b, z)$ represents the clear column transmittance in reference to the cloud base height z_b. However, the clear column transmittances are normally available in reference to the top of the atmosphere; i.e., in the form $\tau_i(\infty, z)$. Thus, values of $\tau_i(z_b, z)$ need to be reevaluated. According to the definition of the spectral transmittance, it is the ratio of the output radiance to the input radiance. Let the input radiance for the first layer be I_0 and the output radiance be I_1, which is also the input radiance for the second layer. If the output radiance for the second layer is I_2, then the transmittance of the combined layer, by definition, can be obtained from the product of the transmittance of the individual layer, i.e., $I_2/I_0 = (I_2/I_1)(I_1/I_0)$. On the basis of this physical argument, the transmittance at a given height below the cloud layer in reference to the top of the atmosphere may be expressed by

$$\tau_i(\infty,z)=\tau_i(\infty,z_b+\Delta z)\tau_i(\Delta z)\tau_i(z_b,z). \quad (4)$$

Differentiating Eq. (4) with respect to z, we obtain

$$d\tau_i(\infty,z)=\tau_i(\infty,z_b+\Delta z)\tau_i(\Delta z)d\tau_i(z_b,z). \quad (5)$$

Upon substituting Eqs. (3)–(5) into Eq. (1), the upwelling radiance is now given by

$$I_i(\infty)=[\tau_i^c(\Delta z)/\tau_i(\Delta z)]\{B_i(T_s)\tau_i(\infty,0) + \int_0^{z_b} B_i[T(z)]d\tau_i(\infty,z)\} + \int_{z_b+\Delta z}^{\infty} B_i[T(z)]d\tau_i(\infty,z). \quad (6)$$

It is apparent that

$$\lim_{\Delta z\to 0} I_i(\infty)=B_i(T_s)\tau_i(\infty,0) + \int_0^{\infty} B_i[T(z)]d\tau_i(\infty,z). \quad (7)$$

This is the transfer equation for the clear column radiance. Eq. (6) represents the fundamental transfer equation to be used for the inference of the temperature profile and cloud parameters.

2.1 Reconstruction of the clear column radiances

In order to formulate iteration procedures for the recovery of the temperature profile, it is assumed that the bulk of upwelling infrared energy in a clear atmosphere arises mainly from the narrow area of the peak of the weighting function. Thus, the clear column radiance may be approximated by

$$I_i(\infty)\approx B[T(z_i)](\partial\tau/\partial z)_i\Delta_i z\,, \qquad (8)$$

where z_i is the selected level at which the contribution of radiant energy to the observed radiance is maximum or substantial, $\partial\tau/\partial z$ denotes the weighting function, and $\Delta_i z$ is the effective width of the weighting function for the ith channel.

For cirrus cloudy conditions, we classify the sounding channels into two groups according to the height of the weighting function peak with respect to that of the cloud. For the weighting functions whose peaks are above or within the cloud layer, the upwelling radiance given in Eq. (6) may be approximated by

$$I_i\approx\frac{\tau_i^c(\Delta z)}{\tau_i(\Delta z)}\eta_i^*+\int_{z_b+\Delta z}^{\infty}B_i[T(z)]d\tau_i(\infty,z), \qquad (9)$$

where

$$\eta_i^*=\int_0^{z_b}B_i[T(z)]d\tau_i(\infty,z). \qquad (10)$$

Assuming that the cloud thickness is relatively thin, we may then write

$$\begin{aligned}&I_i+[1-\tau_i^c(\Delta z)/\tau_i(\Delta z)]\eta_i^*\\&\approx\int_0^{\infty}B_i[T(z)]\,d\tau_i(\infty,z)\\&\approx B[T(z_i)](\partial\tau/\partial z)_i\Delta z_i\,.\end{aligned} \qquad (11)$$

Thus, we obtain the relaxation equation in the form (Chahine, 1970)

$$\frac{\tilde{I}_i'}{I_i^{(n)\prime}}=\frac{B[T^{(n+1)}(z_i)]}{B[T^{(n)}(z_i)]}\,, \qquad (12_a)$$

where

$$\left.\begin{aligned}\tilde{I}_i'&=\tilde{I}_i+[1-\tau_i^c(\Delta z)/\tau_i(\Delta z)]\eta_i^*\\I_i^{(n)\prime}&=I_i^{(n)}+[1-\tau_i^c(\Delta z)/\tau_i(\Delta z)]\eta_i^*\,,\end{aligned}\right\} \qquad (12_b)$$

with n denoting the step of iteration, and $\tilde{I}_i$ represents the observed radiance. But the Planck function is

$$B[T(z_i)]=a\nu_i^3/[\exp(b\nu_i/T)-1]\,, \qquad (13)$$

where ν_i is the wavenumber for the ith channel, and a and b are constants. It follows that

$$T^{(n+1)}(z_i)=b\nu_i/\ln\{1-[1-\exp(b\nu_i/T^{(n)}(z_i))]I_i^{(n)\prime}/\tilde{I}_i'\} \qquad (14)$$

Likewise, for the weighting functions whose peaks are below the cloud, we define

$$r_i^*=\int_{z_b+\Delta z}^{\infty}B_i[T(z)]d\tau_i(\infty,z). \qquad (15)$$

By virtue of Eq. (6), we write

$$\begin{aligned}I_i\approx\frac{\tau_i^c(\Delta z)}{\tau_i(\Delta z)}&[B_i(T_s)\tau_i(\infty,0)\\&+\int_0^{z_b}B_i[T(z)]d\tau_i(\infty,z)]+r_i^*\,.\end{aligned} \qquad (16)$$

Hence, we have

$$\begin{aligned}&(I_i-r_i^*)\tau_i(\Delta z)/\tau_i^c(\Delta z)+r_i^*\\&\approx\int_0^{\infty}B[T(z)]\,d\tau_i(\infty,z)\\&\approx B[T(z_i)](\partial\tau/\partial z)_i\Delta z_i\,.\end{aligned} \qquad (17)$$

In analogy to Eq. (12), the relaxation equation is then

$$\frac{\tilde{I}_i''}{I_i^{(n)\prime\prime}}=\frac{B[T^{(n+1)}(z_i)]}{B[T^{(n)}(z_i)]}\,, \qquad (18_a)$$

where

$$\left.\begin{aligned}\tilde{I}_i''&=(\tilde{I}_i-r_i^*)\tau_i(\Delta z)/\tau_i^c(\Delta z)+r_i^*\\I_i^{(n)\prime\prime}&=[I_i^{(n)}-r_i^*]\tau_i(\Delta z)/\tau_i^c(\Delta z)+r_i^*\end{aligned}\right. \qquad (18_b)$$

In Eqs. (12b) and (18b), the cloud transmissivity is approximated by a simple exponential function to be discussed below. The corresponding clear column transmissivity is obtained by interpolating the known clear column transmissivities. In principle, γ_i^* and η_i^* depend on the temperature profile and iteration schemes can be constructed for these two parameters in the inversion program. However, we found that convergence of the solution becomes very difficult if γ_i^* and η_i^* are changing during numerical experiments. For this reason, γ_i^* and η_i^* are evaluated from the initial guess of the temperature profile. Thus, initial guess plays a significant role in the retrieval program.

2.2 *Computation of the cirrus cloud thickness*

For computation of the cloud thickness, we select a spectral channel in the window region where the effect of water vapor absorption above the cirrus cloud layer normally fairly high in the atmosphere may be neglected. Thus,

$$\int_{z_b+\Delta z}^{\infty} B_i[T(z)]d\tau_i(\infty,z)\approx 0$$

$$\tau_i(\infty,z_b+\Delta z)\approx 1 \qquad (19)$$

Numerical justification of Eq. (19) has been carried out by Liou (1977). In this study we assume that the cirrus cloud base height is designated at 8 km and that the cirrus cloud transmissivity is given by

$$\tau_i^c(\Delta z)=\exp(-\overline{\beta}_e\Delta z) \qquad (20)$$

where $\overline{\beta}_e$ is a prescribed mean extinction coefficient for ice particles. We use a value of 1 km^{-1}, which is a reasonable extinction coefficient for ice crystal clouds in the infrared wavelength. Clearly, the cloud transmissivity expression does not take into account the emission contribution, which is temperature dependent, and therefore it is valid only when cirrus are relatively thin.

With the simplification given in Eq. (19), the upwelling radiance derived in Eq. (6) can be written as

$$I_i=\exp(-\overline{\beta}_e\Delta z)[B_i(T_c)\tau_i^*+I_i] \qquad (21)$$

where

$$\tau_i^*=\tau_i(\infty,0)/\tau_i(\Delta z)$$

$$I_i^*=\int_0^{z_b} B_i[T(z)]d\tau_i(\infty,z)/\tau_i(\Delta z). \qquad (22)$$

Consequently, the relaxation equation for the thickness iteration is given by

$$\frac{\tilde{I}_i}{I_i^{(n)}}\approx\exp\{-\overline{\beta}_e[\Delta z^{(n+1)}-\Delta z^{(n)}]\}. \qquad (23a)$$

Upon rearranging the terms we get

$$\Delta z^{(n+1)}\approx\Delta z^{(n)}-\ln[\tilde{I}_i/I_i^{(n)}]/\overline{\beta}_e \qquad (23b)$$

It is apparent from Eq. (6) that the water vapor profile information is needed to compute the upwelling radiance in the window channel. However, a known water vapor profile from climatology is assumed in this study. Eqs. (12), (18) and (23) form a complete set of basic equations for the simultaneous recovery of the temperature profile and cloud thickness.

3. Computational Analyses and Results

3.1 *Discussion on numerical procedures*

The procedures for numerical iterations involving temperature retrieval used here were based largely on those proposed by Chahine (1972, 1974). Some relevant aspects of the relaxation method will be discussed briefly in this section.

Eq. (14) transforms changes in the ratio $\tilde{I}_i/I_i^{(n)}$ at different points on the wavenumber-axis into changes in $T^{(n)}(z_i)$ at specific points along the height-axis. The mechanism of this transformation is iterative in which $T^{(n)}(z_i)$ is modified at every step n to yield a new value $T^{(n+1)}(z_i)$. We may write the relaxation transformation in the form

$$T^{(n+1)}(z_i)=\alpha_i^{(n)}T^{(n)}(z_i), \qquad (24)$$

where $\alpha_i^{(n)}$ are scaling factors, which may be obtained by substituting the Planck function in explicit form into Eqs. (12) and (18). Thus, the scaling factors can be shown to be

$$\alpha_i^{(n)}=\frac{b\nu_i/T^{(n)}(z_i)}{\ln\{1-[1-\exp(b\nu_i/T^{(n)}(z_i))]I_i^{(n)\prime}/\tilde{I}_i'\}} \qquad (25)$$

The interations of the computation start from an initial guess of $T^{(n)}(z_i)$ (i.e., $n = 0$) and terminate by checking the residuals

$$R^{(n)} = \frac{1}{J}\left\{\sum_{i=1}^{J}\left[\frac{\tilde{I}_i' - I_i^{(n)\prime}}{\tilde{I}_i'}\right]^2\right\}^{1/2} \qquad (26)$$

If $R^{(n)} \to 0$, or is smaller than a certain criterion value, then $I_i^{(n)\prime}$ is a solution. In Eq. (26), J is the total number of channels for the temperature retrieval.

It is sometimes necessary to use a weighted form of the scaling factors because convergence to a solution may be affected by random errors in measurements, which cause the residuals to diverge from zero. The residuals first decrease and then approach an asymtotic value having the same order of magnitude as the errors in the observed values. This behavior is due to the partial overlapping of the kernels and it suggests that the iterative process should be terminated when $R^{(n)}$ approaches its asymtotic value. Beyond this point iterations do not necessarily extract the further information of the temperature field from the data, and in the presence of large noise levels in the measurements, the additional iterations might lead to oscillations in the recovered solutions. To prevent such oscillations, it was suggested by Chahine (1972) to apply, after a few iterations, say $n > 3$, certain weights to the scaling coefficients, the so-called weighted scaling factors $\bar{\alpha}_i^{(n)}$. The use of $\bar{\alpha}_i^{(n)}$ will slow down the rate of convergence considerably but it will tend to reduce the effects of random noise in the data in the iterative solution. More details on the convergence properties of the iterative solution can be found in papers by Barcilon (1975) and Chahine (1970, 1972, 1974).

The perturbation approach is especially well suited for problems in which a prior knowledge of the solution is given. For this study, climatological data was used as a first guess to the shape of the solution. To preserve the shape in subsequent iterations, we perform the interpolation on the scaling factors $\alpha_i^{(n)}$ and generate scaling factors $\alpha_{int}^{(n)}(z)$ at all intermediate values of z. The complete interpolated solution is then obtained at all values of z as

$$T^{(n+1)}(z) = \alpha_{int}^{(n)}(z)\, T^{(n)}(z) \qquad (27)$$

It is apparent that the same interpolation procedure can be performed when $\bar{\alpha}_i^{(n)}$ is used. In this process, the final answer is made to depend on the initial guess by preserving the form of the input function $T^{(0)}(z)$ in all of the steps of the iterative solution.

The present relaxation method of solution is a discrete numerical process in which convergence is judged by the extent to which the algorithm suppresses the effects of quadrature, random, and systematic errors on the final temperature profiles. More information regarding the uniqueness and stability of the solution can be found in the work by Chahine (1970, 1972, 1974), and Twomey (1977).

3.2 Characteristics of Nimbus 6 HIRS channels and data selections

The Nimbus 6 satellite was launched in June 1975. It is a sun-synchronous polar orbiting satellite with a height of 1,100 km and having local noon (ascending) and midnight (descending) equator crossing. Successive orbits cross the equator with 26.8 degrees of longitude separation and the orbital period is about 107.25 min. The Nimbus 6 HIRS instrument is a third-generation infrared radiation sounder. The instrument scans perpendicular to the satellite subtrack. There are 42 scan spots per scan line with a resolution of 23 km near nadir and 31 km at the extremes of the scan. The HIRS instrument senses infrared radiation in 17 channels, which include seven channels in the 15 μm CO_2 band, five channels in the 4.3 μm CO_2 band, water vapor channels at 6.8 and 8.6 μm, and three channels in the windows at 11, 3.68 and 0.69μm.

The data that are routinely processed at NOAA/NESS are available on nine-track, 1600 bpi tapes. The data are packed in such a way that six or seven orbits are available on each tape. These tapes contain co-located and calibrated radiance values for all 17 channels (Smith *et al.*,

1975). The data set used in this analysis was for the period during 20-30 August 1975, during which all channels of HIRS instrument were operating properly. The data cover a geographical area from 80-150°W and 20-50°N from which a number of numerical experiments were carried out. However, we have selected August 25 data for the comprehensive comparisons between the resulting numerical experiments and the synoptic observations and satellite photographs. The Nimbus 6 satellite track over the central North America on 25 August is marked by the arrow on the weather map shown in Fig. 1. The satellite passed over

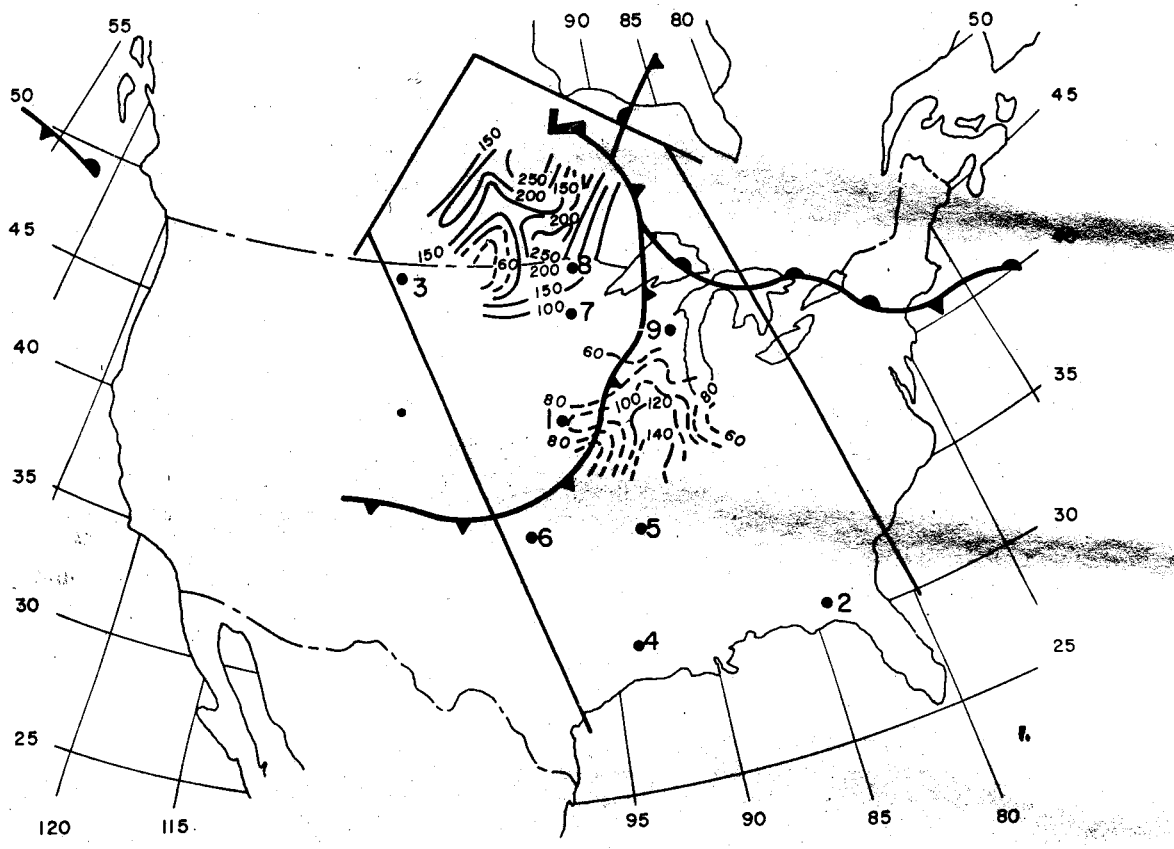

Fig. 1. Surface weather map for August 25, 1975, 12Z in which the frontal position is shown. The arrow indicates the Nimbus 6 satellite track on this date. Also shown are the cloud ice and water content (g m^{-2}) based on empirical-theoretical calculations (Feddes and Liou, 1978). Dotted and solid lines are for cirrus and middle clouds, respectively. The black dots and numerical numbers denote the stations selected for inversion experiments.

the southern boundary of the United States at about 17:16Z, and left the northern edge of the low pressure center as shown in the weather map at about 17:23Z. The synoptic conditions on 25 August will be discussed in the following section.

In numerical computations, the simulated atmosphere was divided in such a way that it coincided with the pressure levels used in the clear column radiance program (CCR) developed at NOAA/NESS and kindly provided to us by Smith (private communication). There are 40 pressure levels for the CCR program. The program utilizes predetermined transmission

profiles which can be empirically adjusted as a function of the climatological temperature and moisture profiles. The weighting functions for the HIRS channels are depicted in Fig. 2. The

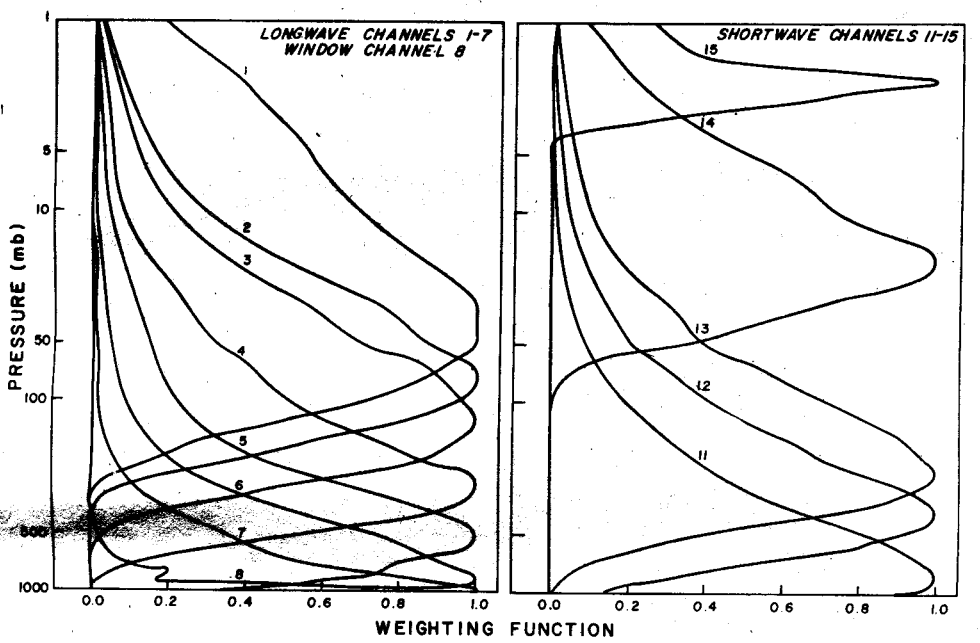

Fig. 2. The weighting functions of the HIRS longwave, shortwave and window channels based on mid-latitude summer climatological data.

peak in the figure indicated the approximate location in the atmosphere from which most of its energy is derived.

We have used 13 HIRS channels including seven in the 15 um Co_2 band and five in the 4.3 μm CO_2 band for the temperature iterations, and one in the window for the cloud thickness iterations. We have included the CO_2 shortwave channels in the study to investigate if the addition of these channels may improve the resolution of the temperature profile in the retrieval. Shown in Fig. 3 are comparisons between the resulting temperature retrievals with and without the shortwave channels for the Miami case where clear conditions were reported on 22 August. The comparisons reveal that the retrieval computations including shortwave channels improve the resolution of the temperature profile above the tropopause. Moreover, Fig. 3 also illustrates that the iterations with shortwave channels included give a 1.1°K mean temperature error as compared with the radiosonde observations, whereas a 2.7°K mean temperature error is found when only the longwave channels are employed in the experiments.

3.3 Numerical experiments using HIRS data for cloudy cases

In the preliminary simulation study by Liou and Yeh (1978), mid-latitude summer climatological humidity and temperature profiles were used as a model profile and various cloud thickness were inserted in the atmosphere to evaluate the expected upwelling radiance. The temperature profile and cirrus cloud thickness were retrieved utilizing the expected upwelling radiance with various random errors added. The synthetic experiments showed that the average deviations of the temperature profile increase with increasing random errors. The mean temperature errors evaluated at each 50 mb interval were about 1.3°, 1.4° and 1.8°K for the 0.5 km cirrus case and about 1.3°, 1.5° and 1.9°K for the 1 km cirrus case involving random

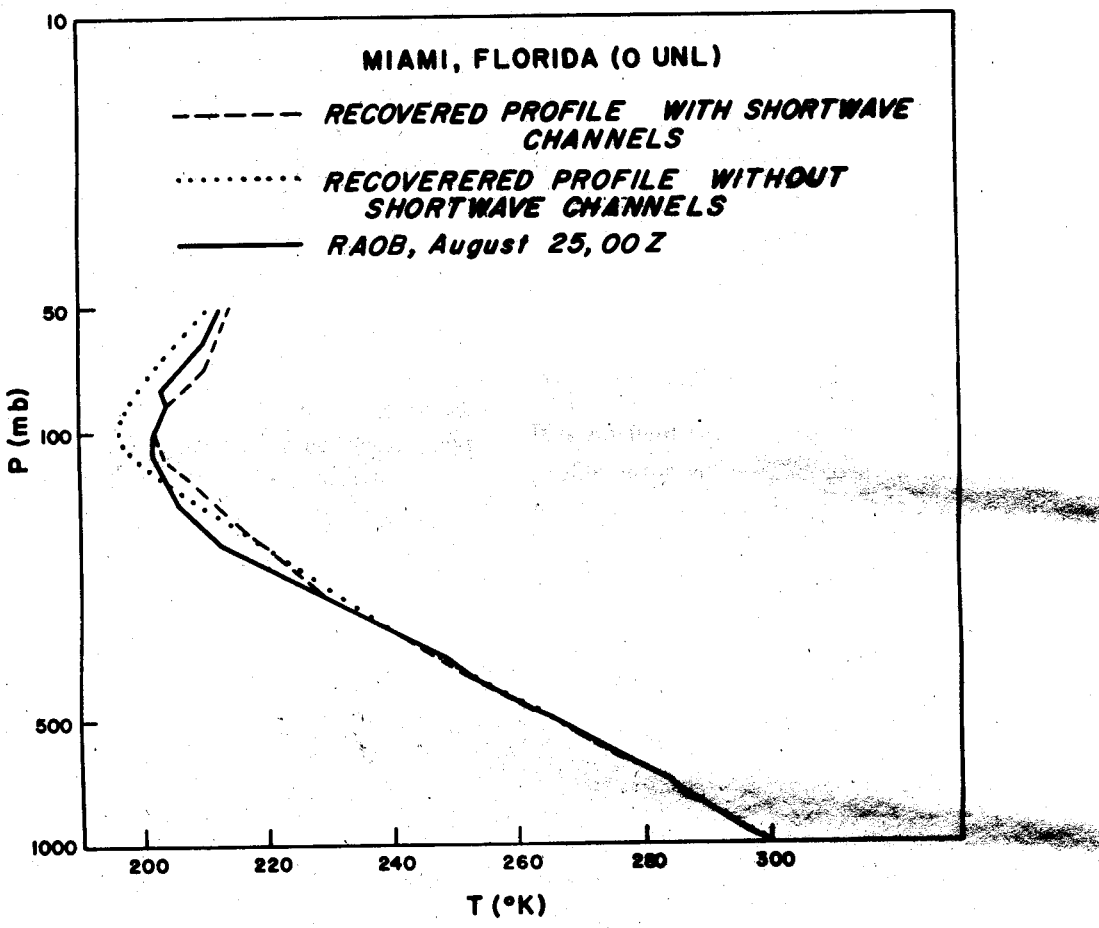

Fig. 3. Temperature profile retrievals with and without including the 4.3 μm CO_2 band from HIRS radiances for the Miami case on August 22, 1975, 18Z.

errors of 0,2 and 4%, respectively. The retrived clear column temperature profile also reveals similar errors.

Upon utilizing the available HIRS radiance data during 20-30 August 1975, a number of cases with different synoptic situations were chosen to perform the retrieval exercises. In this paper we will only present cases on 25 August along with the corresponding synoptic observations and GOES satellite IR picture. On 25 August, there was a deep low pressure in the northern central portion of the North America. The cold front extended from the low center in central Canada to mid-west of the United States. Middle clouds were present from 53° N, 97.5°W to 47°N, 84.5°W and cirrus clouds from 44°N, 93°W to 39°N, 91.7°W on this date as shown in Fig. 1. The dotted and solid lines in this figure represent the vertical liquid content of cirrus and middle clouds (g m^{-2}), respectively, derived by Feddes and Liou (1978) on the basis of theoretical-empirical analyses. Analyses of the satellite photograph and synoptic reports also indicated that the southern cloud area was composed of cirrus on top of an active area of thunderstorms. The northern cloud area, which was over the southern Canada and extended to the northern Montana and North Dakota, was dominated by middle clouds with some cirrus on the southwest side. As evidenced from the satellite picture, clouds were not present in the south portion of the United States.

By examining the synoptic reports and

GOES satellite IR picture (Fig. 4), nine stations with various sky conditions were selected for the purpose of numerical experiments on the temperature profile and cloud thickness retrie-

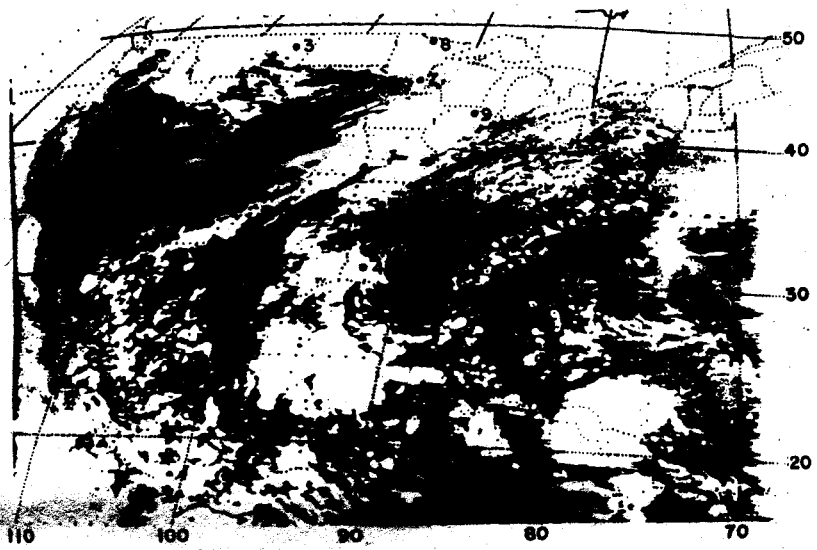

Fig. 4. GOES IR picture for August 25, 1975.

val. The chosen stations are marked according to the numerical order from 1 to 9 as shown in Fig. 1. The observed cloud coverage and the height of the nine stations are listed in the first two columns of Table 1, while the last two columns give the results derived from the numerical computations. It is evident that the first four cases involve single layers of high thin cirrus. Cases 5, 6, and 7 consist of no cloud, and the last two cases are seen to be covered by low clouds or layered clouds. Below we describe the representative cases in each category in conjunction with the numerical experiments on the temperature profile and cloud thickness retrieval.

Table 1. The synoptic observations and the resulting inversion computations for the cloud thickness and mean temperature errors for the nine selected weather stations.

Index	Station	Sky Coverage (tenths)	Ceiling Height (X 100 ft)	Retrieved Cloud Thickness (km)	Mean Temperature Error Below 30 mb (K°)
1	Omaha, Neb.	7	250	0.95	1.6
2	Apalachicóla, Fla.	6	250	0.02	2.0
3	Glasgow, Mont.	8	UNL*	0.53	2.5
4	Lake Charles, La.	9	250	0.12	2.0
5	Little Rock, Ark.	5	UNL	0.05	2.7
6	Oklahoma City, Okla.	0	UNL	0.04	2.3
7	St. Cloud, Minn.	0	UNL	0.00	1.3
8	International Falls, Minn.	9	35	0.30	3.3
9	Green Bay, Wisc.	10	25	0.45	2.0

*UNL implies that the ceiling height is unlimited.

Fig. 5 shows the recovered temperature profile and cirrus cloud thickness, along with the mid-latitude summer climatological temperature profile used as initial guess for the Omaha case

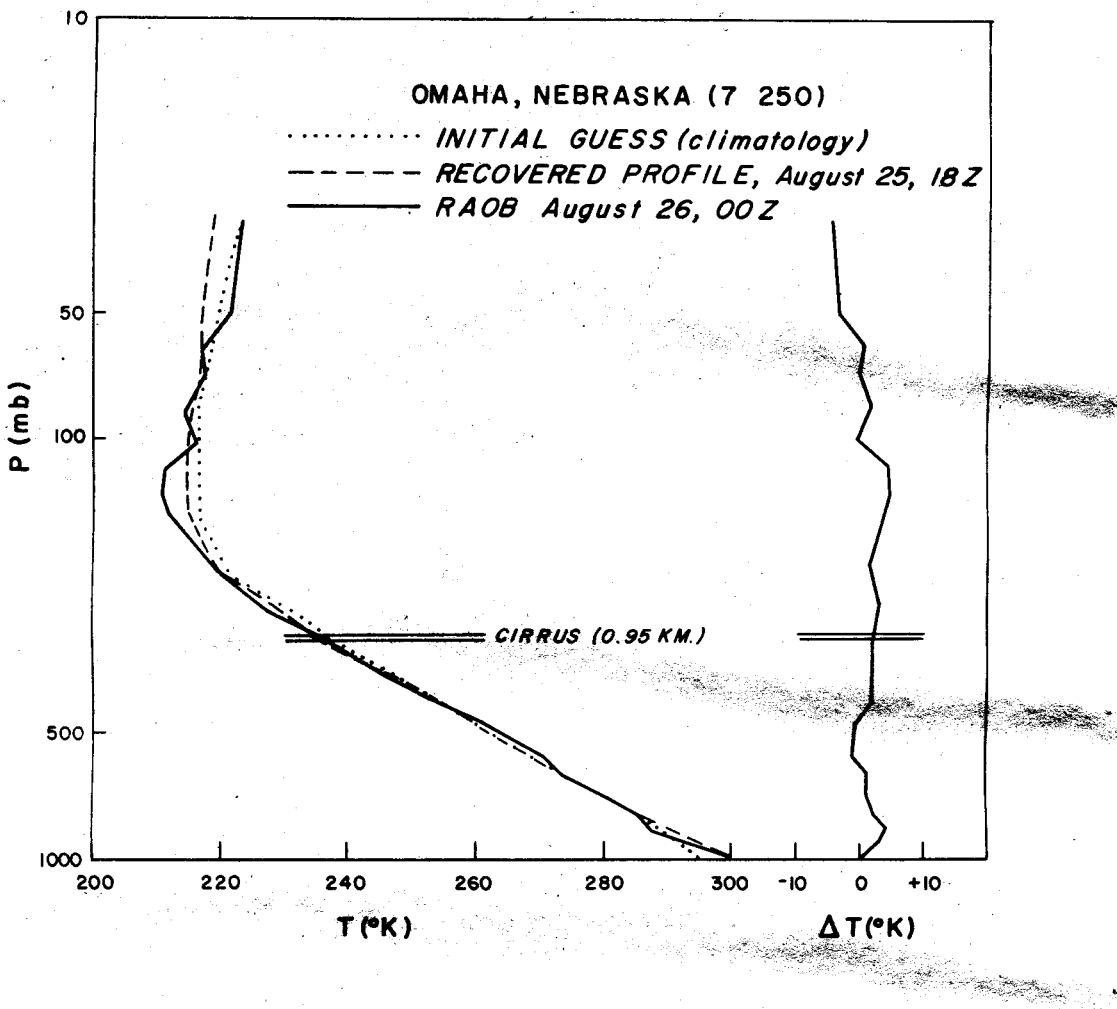

Fig. 5. Temperature profile and cirrus cloud thickness retrieved from HIRS radiances on August 25, 1975, 18Z for Omaha case in which only single cirrus layer was observed.

(the first category, thin cirrus alone). The radiosonde sounding at 00Z on 26 August is also plotted for comparison purposes. The recovered temperature profile in general compares well with the observed soundings up to the tropopause. Above 200 mb, the shape of the recovered temperature profile is similar to that of the initial guess profile due to the modified relaxation method used in this study as mentioned in the previous section. The retrieved cloud thickness is about 0.95 km using an extinction coefficient of 1 km^{-1} This value also agrees well with that derived by Feddes and Liou (1973) using a combination of HIRS channels by means of a theoretical-empirical method. It should be pointed out that there is no objective means to verify the derived cloud thickness in the present study since the surface weather report only gives the ceiling height of the cloud. Even if the cloud thickness information were available, say, from the aircraft report, it would be difficult to have a reasonable comparison since in the numerical experiments, a fixed cloud base height was assumed. In any

event, the reliable cloud composition information might have to be derived from a separate cloud sounding program.

The recovered temperature profile for the Oklahoma City case (the second category, clear) shown in Fig. 6 is found to match quite closely

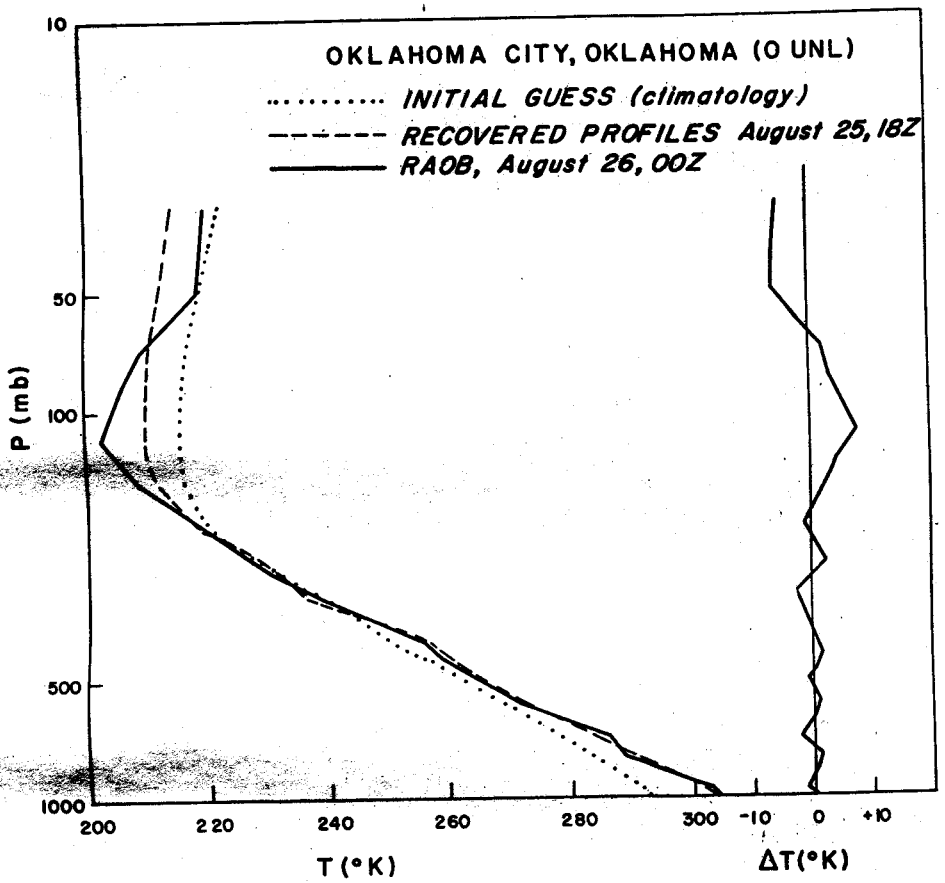

Fig. 6. Same as Fig. 5, except for Oklahoma City where clear condition was reported.

the radiosonde observations in the troposphere. The preservation of the shape of the initial guess and the lacking of sounding channels near and above the tropopause prevent the numerical solution from approaching the observed sounding profile in the lower stratosphere. The retrieved cloud thickness in this case is 0.04 km, which is negligibly small for all practical considerations.

In Fig. 7, we present the International Falls case corresponding to the final category (multilayered clouds). We note that based on the radiosonde observations a strong temperature inversion was present below the cloud. The inversion causes a great deal of difficulties in retrieving the temperature profile. However, the temperature profile obtained appears to be reasonable in the lower portion of the atmosphere, even in the presence of low cloud and strong inversion. The recovered temperature profile above 400 mb reveals unsatisfactory fluctuations probably caused by the presence of the low cloud deck. As for the cloud thickness,

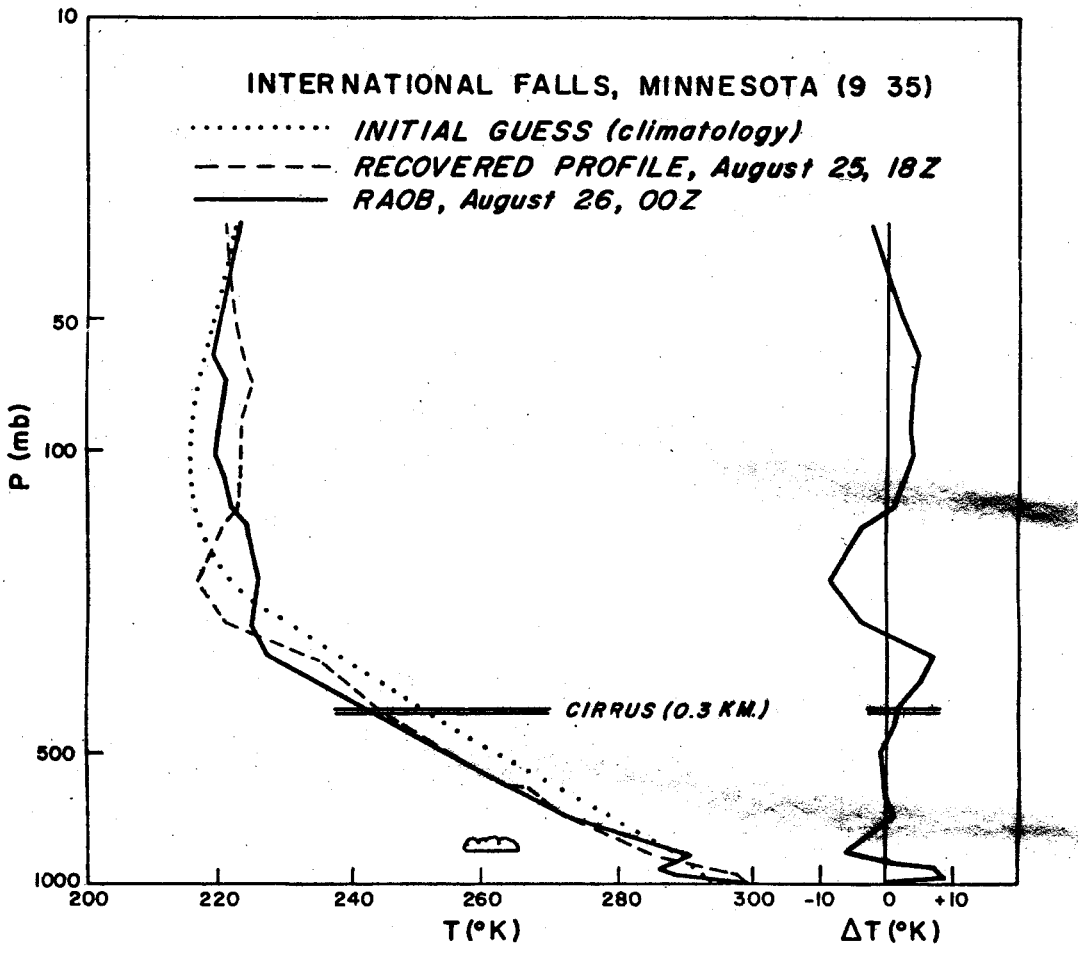

Fig. 7. Same as Fig. 5, except for International Falls where layered clouds were observed.

there is no available observed data to verify whether the retrieved cloud thickness of 0.30 km is a reliable value.

4. Concluding Remarks

A modified relaxation method for the simultaneous recovery of the temperature profile and cloud thickness has been developed based on the parameterized infrared radiative transfer equation for cloudy atmospheres. Numerical experiments have been carried out utilizing Nimbus 6 HIRS data in which three basic sky conditions were chosen. These conditions include cirrus alone, clear and multilayered clouds. Numerical results show that for cases involving thin cirrus alone, the retrieved temperature profiles are as accurate as those recovered in clear atmospheres. Moreover, cloud thicknesses derived from the relaxation program are generally in good comparison with those obtained from the synoptic report and satellite cloud picture. However, the temperature inversion program when multilayered clouds are involved has been shown to be unsatisfactory. We also found that one serious problem encountered in the inversion of satellite radiance data to yield temperature information was the significant variability of radiance values for locations not far apart, due, probably, to the instrumentational error. The possible error in the measured radiance frequently prevents the convergence of the solution. The measurement error effect is more profound than the numerical iteration scheme in which the clear column radiance is reconstructed.

Because of the different cloud conditions and combinations to be anticipated in the changing atmosphere, it seems not feasible to have a universal algorithm for the recovery of the temperature profile and cloud property simultaneously. A separate and parallel program for the determination of cloud composition and structure from sounding channels may be required in order to derive realistic temperature profiles in all weather conditions.

ACKNOWLEDGEMENTS

This research was supported, in part, by the Air Force Geophysics Laboratory under contract F19628-78-C-0144. We thank Drs. Fleming and Chahine for helpful comments on this paper.

REFERENCES

Bhartia, V., 1975: Chahine's relaxation method for the iterative transfer equation. *J. Atmos. Sci.*, 32, 1626-1630.

Chahine, M. T., 1970: Inverse problems in radiative transfer: Determination of atmospheric parameters. *J. Atmos. Sci.*, 27, 960-967.

Chahine, M. T., 1972: A general relaxation method for inverse solution of the full radiative transfer equation. *J. Atmos. Sci.*, 29, 741-747.

Chahine, M. T. 1974: Remote sounding of cloudy atmospheres. I. The single cloud layer. *J. Atmos. Sci.*, 31, 233-243.

Feddes, R. G. and K. N. Liou, 1978: Atmospheric ice and water content derived from parameterization of Nimbus 6 High Resolution Infrared Sounder data. *J. Appl. Meteor.*, 17, 536-551.

Liou, K. N., 1977: Remote sensing of the thickness and composition of cirrus clouds from satellites. *J. Appl. Meteor.*, 16, 91-99.

Liou, K. N., and H. Y. Yeh, 1979: Remote sounding of the temperature profile and cloud thickness in cirrus cloudy atmospheres from Nimbus VI HIRS channels. *Space Research, XVIII*, 157–160.

Roewe, D. and K. N. Liou, 1978: Influence of cirrus clouds on the infrared cooling rate in the troposphere and lower stratosphere. *J. Appl. Meteor.*, 17, 92-106.

Smith, W. L., 1970: Iterative solution of the radiative transfer equation for the temperature and absorbing gas profile of an atmosphere. *Appl. Opt.*, 9, 1993-1999.

Smith, W. L., H. M. Woolf and W. J. Jacob, 1970: A regression method for obtaining real time temperatures and geopotential height profiles from satellite spectrometer measurements and its application to Nimbus 3 SIRS observations. *Mon. Wea. Rev.*, 98, 582-594.

Smith, W, L., P. G, Abel, H. M Woolf, A. W. McCulloch and B. J. Johnson, 1975: The high resolution infrared radiation sounder (HIRS) experiment. *Nimbus VI Users Guide*, Goddard Space Flight Center, Greenbelt, Md., 227 pp.

Twomey, S., 1977: *Introduction to the Mathematics of Inversion in Remote Sensing and Indirect Measurements.* Elsevier, New York, 179 pp.

卷雲大氣中溫度剖面及雲厚度倒求之數值實驗

葉 華 陽　　廖 國 男

美 國 猶 他 大 學 氣 象 系

本文是以參數化的紅外線輻射方程式爲基礎，發展漸近法來解密卷雲大氣中溫度剖面及雲厚度的倒求問題。在這研究中，我們利用雨雲六號(Nimbus 6)之高鑑別紅外線探測儀器(High Resolution Infrared Sounder)的資料包括二氧化碳長和短波頻道來做溫度剖面及雲厚度之修正實驗及數值分析。倒求的數值結果曾就物理意義上討論並且和雷送觀測資料相比較。比較中顯示出在薄卷雲的狀況下，從衛星資料倒求的溫度剖面與觀測資料相當接近。但是當有中低雲出現時，倒求的溫度剖面與觀測值比較則顯出不規則的波動，而雲厚度計算值的精準度也無法確定。